



## Construction and characterization of a rotating cylinder electrode for different technological applications

J.M. MACIEL<sup>1,2</sup> and S.M.L. AGOSTINHO<sup>2</sup>

<sup>1</sup>*Instituto de Química, Universidade de São Paulo. Av. Prof. Lineu Prestes 748, Caixa Postal 26077, CEP 05908-970, São Paulo – SP, Brazil;*

<sup>2</sup>*Departamento de Ciências Farmacêuticas, Universidade de Marília. Av. Prof. Higino Muzzi Filho, 1001, CEP 17525-902, Marília – SP, Brazil*

Received 11 December 1997; accepted in revised form 23 October 1998

**Key words:** copper–nickel alloys, corrosion, electrochemistry, rotating cylinder electrode

### Abstract

A rotating cylinder electrode (RCE) for corrosion studies has been constructed and hydrodynamically characterized. Empirical hydrodynamic parameters were determined from limiting current density and weight loss measurements for four different electrochemical processes. Statistical data analysis established the confidence limits of these parameters.

### List of symbols

$A$  electrode area (cm<sup>2</sup>)  
 $C$  concentration (mol dm<sup>-3</sup>)  
 $d$  electrode diameter (cm)  
 $D$  diffusion coefficient (cm<sup>2</sup> s<sup>-1</sup>)  
 $F$  Faraday's constant (C mol<sup>-1</sup>)  
 $f$  frequency (s<sup>-1</sup>)  
 $i_L$  limiting current density (A cm<sup>-2</sup>)  
 $k, k_1$  constants  
 $n$  number of electrons involved in a redox process  
 $Re$  Reynolds number ( $Ud/\nu$ )

$r_1$  inner radius  
 $r_2$  outer radius  
 $Sc$  Schmidt number, ( $\nu/D$ )  
 $Ta$  Taylor number (see text)  
 $Ta^*$  modified Taylor number (see text)  
 $x$  constant  
 $U$  electrode peripheric velocity (cm s<sup>-1</sup>)  
 $\delta_N$  Nernst diffusion layer thickness (cm)  
 $\delta_{Pr}$  Prandtl hydrodynamic layer thickness (cm)  
 $\nu$  kinematic viscosity (cm<sup>2</sup> s<sup>-1</sup>)  
 $\omega$  angular velocity of electrode (rad s<sup>-1</sup>)

### 1. Introduction

The rotating cylinder electrode (RCE) offers an interesting alternative for electrochemical studies in that it has simple construction, reproducible response and reaches the turbulent flow condition at low Reynolds numbers. Its application in corrosion studies for example, permits the use of samples in the form of tubes, simulating the hydrodynamic conditions in which the material is commonly employed.

The lack of an exact mathematical solution for the turbulent flow case has been responsible for the empirical approach used to describe mass transport at a RCE surface. Eisenberg, Tobias and Wilke [1] were the first to

carry out a detailed investigation on mass transport to RCE under turbulent flow. From measurements of limiting current density at a smooth Ni RCE using the Fe(CN)<sub>6</sub><sup>3-</sup>/Fe(CN)<sub>6</sub><sup>4-</sup> couple in alkaline medium they obtained:

$$i_L = knFCd^{-0.3}\nu^{-0.344}D^{0.644}U^x \quad (1)$$

where  $k = 0.0971$  and  $x = 0.7$ .

Pang and Ritchie [2] minimized the end effects by installing inert ends and obtained the following equation:

$$i_L = knFCd^{-0.299}\nu^{-0.345}D^{0.644}U^x \quad (2)$$

where  $k = 0.086$  and  $x = 0.71$ .

Gabe and Walsh [3, 4] obtained the value  $x = 0.74$  from cupric ion electroreduction to metallic copper on a smooth cylinder and observed that  $x$  changes to 0.9 as the electrode surface becomes rougher. The RCE has also been used in corrosion studies [5–7] and in the determination of diffusion coefficients in molten salts [8].

The effect of roughness and geometry on experimental  $x$  and  $k$  values are discussed in the literature [3, 4, 9, 10] but each author is interested in a particular system. Studies concerning different processes on the same surface, in order to evaluate the confidence limits of these transport parameter values, are lacking.

The aim of this work is to describe the construction of an RCE and to determine its hydrodynamic characteristics from its performance in different electrochemical processes: metal electrodeposition, corrosion studies, and limiting current density measurements on inert electrodes, where different roughness levels are observed. In other words, the  $x$  and  $k$  values will be determined using the same RCE and different electrochemical systems.

## 2. Experimental details

The RCE is shown in Figure 1. It is composed of an AISI 304 stainless steel shaft (a) with a thread (b) at one end. This shaft was machined on a lathe from a rod of larger diameter so that a ring (c) was formed at a suitable distance from the threaded end to support the electrode body. The active part (d) comprised a piece of a 90/10 CuNi alloy carefully machined so that the ends were perpendicular to the electrode axis. Typical dimensions were 2.7 cm length and 2.7 cm diameter. Two pieces made of Teflon™ (e) with the same diameter as the electrode body were used for alignment of the active part and to maintain the ends inert. The lower part was threaded on the inside so that when mounted, it provided a tight assembly and prevented access of the electrolyte to the interior of the active part. Electrical contact was achieved by two springs (f) held by a pin fitted in a hole in the shaft. The whole assembly when mounted forms a regular and well-aligned body, without discontinuities. It is easy assembled and allows quick substitution of the active part when necessary. The RCE was connected to an electrical motor through a longitudinal hole in the axis of the later and fixed by bolts. The motor was connected to a power source and the rotation rate varied by discrete values. The rotation rates used were 34, 76, 100 and 226  $\text{cm s}^{-1}$ . An SCE was used as reference electrode, and was fitted to the electrolytic cell by a Luggin probe.

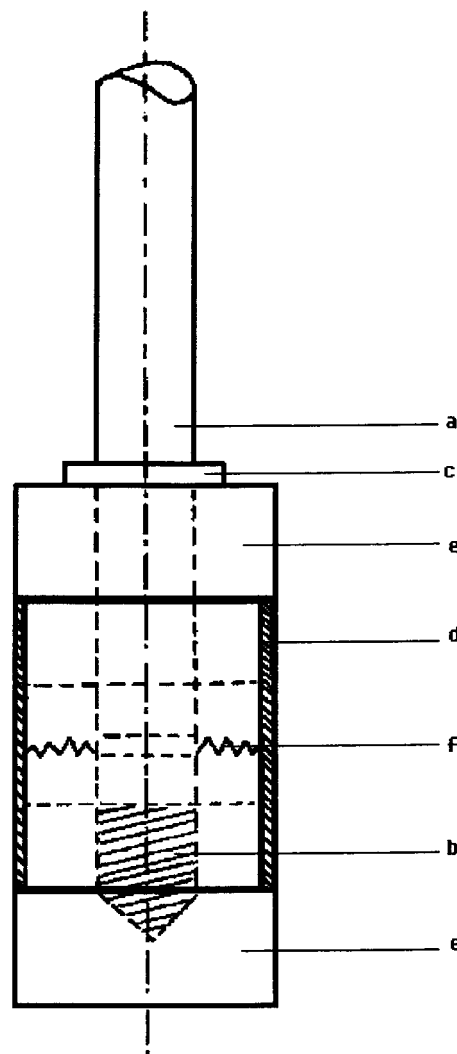


Fig. 1. Rotating cylinder electrode employed in this work. Key: (a) shaft; (b) thread; (c) ring; (d) active part; (e) Teflon™ holders; (f) springs for electrical contact.

A copper foil ( $\text{Cu} \geq 99.9\%$ ), 0.05 cm thickness and 149  $\text{cm}^2$  area was used as counter electrode in copper electroreduction. This foil was curved in the form of a hemicylinder with 4.5 cm inner radius. In  $\text{Fe}^{3+}/\text{Fe}^{2+}$  reduction limiting current density measurements the counter electrode was a 5 cm diameter and 5.5 cm height cylindrical platinum gauze. The working electrode was polarised using an Aardvark PEC 1 potentiostat.

All experiments were conducted in a water-jacketed electrolytic cell with a gas purging system. The electrolyte was deaerated during 40 min before each experiment. Nitrogen gas, purified as described elsewhere [11] was used for electrolyte deaeration. All measurements were conducted at  $(25 \pm 1)^\circ\text{C}$  and solutions were

prepared from analytical grade reagents and bidistilled water.

The active surface of the working electrode was sanded with 400 and 600 grit sandpaper and washed with distilled water. After that, it was immersed in the supporting electrolyte for 10 to 20 min, then washed with distilled water and ethanol and dried with hot air.

In a series of experiments, the  $\text{Fe}^{3+}/\text{Fe}^{2+}$  reduction limiting current density was measured on the precorroded active surface of the RCE. The electrode previously prepared was immersed in  $1.0 \text{ mol dm}^{-3}$  HCl/ $16 \text{ mmol dm}^{-3}$   $\text{Fe}^{3+}$  solution for 30 min while rotating at a rate of  $30 \text{ cm s}^{-1}$ . After the corrosion process, the electrode was removed from the solution, rinsed with distilled water and, without drying, immersed in the electrolytic cell where the experiment was started.

### 3. Results and discussion

#### 3.1. Limiting current density measurements

Limiting current density as function of rotation rate of the electrode was measured with the following systems:

- $\text{Cu}^{2+}/\text{Cu}^0$  reduction in  $0.1 \text{ mol dm}^{-3}$   $\text{K}_2\text{SO}_4$  solution with the electrode held at  $-300$ ,  $-400$  and  $-500 \text{ mV vs SCE}$ ;
- $\text{Fe}^{3+}/\text{Fe}^{2+}$  reduction in  $1 \text{ mol dm}^{-3}$  HCl solution with the RCE polarized at  $-350$ ,  $-400$  and  $-450 \text{ V vs SCE}$ ;
- $\text{Fe}^{3+}/\text{Fe}^{2+}$  reduction in  $1 \text{ mol dm}^{-3}$  HCl solution on RCE previously corroded and polarized at  $-400$ ,  $-420$  and  $-440 \text{ mV vs SCE}$ .

For these measurements,  $\text{Cu}^{2+}$  concentration varied between  $0.5$  and  $20 \text{ mmol dm}^{-3}$  and the  $\text{Fe}^{3+}$  concentration between  $0.25$  and  $0.8 \text{ mmol dm}^{-3}$ .

Potential values were defined from potentiostatic polarisation curves previously obtained on the respective media. Some of these results are presented in Figures 2 and 3. The current density values for the  $\text{Fe}^{3+}/\text{Fe}^{2+}$  couple were corrected from subtraction of the limiting current density due to  $\text{O}_2/\text{H}_2\text{O}$  reduction, obtained at the same potential values in the absence of  $\text{Fe}^{3+}$  ions in the electrolyte. This correction was necessary because both platinum auxiliary electrode and RCE were in the same solution.

#### 3.2. Weight loss experiments

Weight loss experiments with the CuNi 90:10 alloy were made in  $1.0 \text{ mol dm}^{-3}$  HCl solution containing  $5$ ,  $10$  and  $16 \text{ mmol dm}^{-3}$  of  $\text{Fe}^{3+}$  ions as oxidant. The weight loss values were converted to current values through

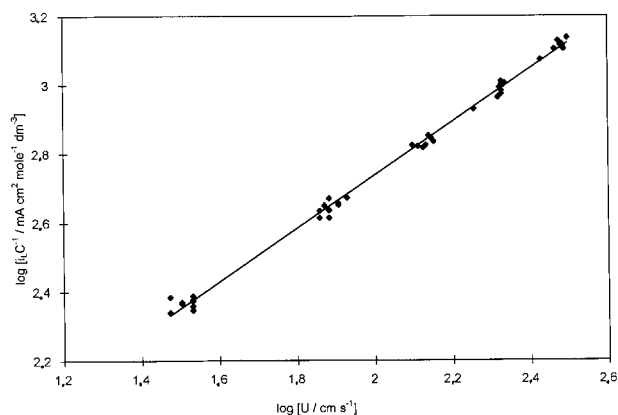


Fig. 2. Limiting current density measurements for  $\text{Cu}^{2+}/\text{Cu}^0$  reduction.  $[\text{Cu}^{2+}] = 0.5 \text{ mmol dm}^{-3}$  in  $0.5 \text{ mol dm}^{-3}$   $\text{K}_2\text{SO}_4$ .

Faraday's law, assuming nonselective dissolution. The results are presented in Figure 4.

#### 3.3. Evaluation of the hydrodynamic parameters

Hydrodynamic parameters were evaluated from the relation between the experimental limiting current density and the rotation rate of the RCE, assumed to obey the equation:

$$i_L = k_1 U^x \quad (3)$$

In its logarithmic form:

$$\log i_L = \log k_1 + x \log U \quad (4)$$

where  $k_1 = knFCAd^{-0.3}v^{-0.344}D^{0.644}$  according to Eisenberg and others [1].

Table 1 presents  $x$  (slopes) and  $k$  (intercepts) values within 95% confidence level obtained in this way.

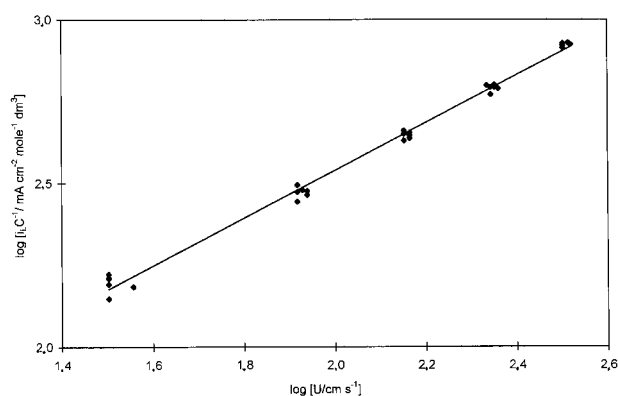


Fig. 3. Limiting current density measurements for  $\text{Fe}^{3+}/\text{Fe}^{2+}$  reduction.  $[\text{Fe}^{3+}] = 0.8 \text{ mmol dm}^{-3}$  in  $1.0 \text{ mol dm}^{-3}$  HCl.

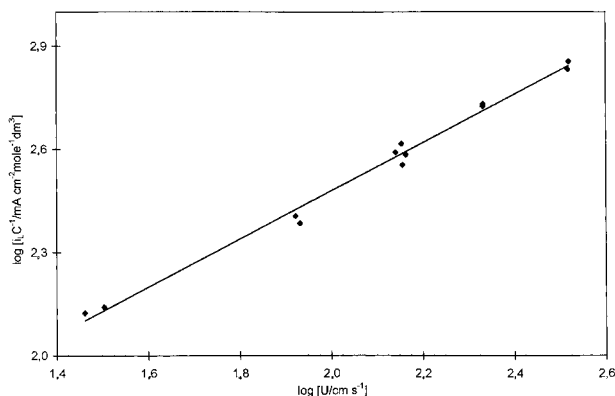


Fig. 4. Weight loss measurements of CuNi 90:10 alloy in HCl/Fe<sup>3+</sup> medium. [Fe<sup>3+</sup>] = 9 mmol dm<sup>-3</sup> in 1.0 mol dm<sup>-3</sup> HCl.

Analysis of variance was applied to the four groups of measurements and showed no differences among them at 99% significance level. The average values are  $k = (0.082 \pm 0.001)$  and  $x = (0.732 \pm 0.001)$  within 95% confidence level. From these results the limiting current on the RCE constructed can be written as

$$I_L = 0.082 n F C a d^{-0.3} \nu^{-0.344} D^{0.644} U^{0.732} \quad (5)$$

### 3.4. Flow regime during the operation of the RCE

The hydrodynamic regime of the RCE can be characterised by the Taylor number [12–14]:

$$Ta = Re[(r_2 - r_1)/r_1]^{1/2} \quad (6)$$

Thus, for  $Ta < 41.3$  the flux is laminar and for  $Ta > 400$  the flux is turbulent. For  $Ta$  between 41.3 and 400 there

Table 1.  $x$  and  $k$  values for the RCE constructed

Experiment type	$x$	$k$
Copper electroreduction	$0.737 \pm 0.018$	$0.075 \pm 0.008$
Weight loss in HCl/Fe <sup>3+</sup>	$0.751 \pm 0.005$	$0.062 \pm 0.001$
Fe <sup>3+</sup> ion reduction on non corroded RCE	$0.750 \pm 0.004$	$0.071 \pm 0.002$
Fe <sup>3+</sup> ion reduction on precorroded RCE	$0.691 \pm 0.002$	$0.118 \pm 0.007$
Average	$0.732 \pm 0.001$	$0.082 \pm 0.001$

Table 2. Hydrodynamic conditions for RCE

rpm	$f$ /Hz	$\omega$ /rad s <sup>-1</sup>	$U$ /cm s <sup>-1</sup>	$\delta_N$ /cm	$\delta_{Pr}$ /cm	$Re$ /10 <sup>-3</sup>	$Ta$ /10 <sup>-3</sup>	$Ta^*$
240	4	25	33.9	0.0033	0.040	9.8	16.2	1687
540	9	56	76.3	0.0019	0.022	22.1	36.6	2821
960	16	100	136.7	0.0014	0.014	39.6	65.6	4033
1500	25	157	212.1	0.0009	0.010	61.5	101.8	5293
2160	36	226	305.4	0.0007	0.008	88.6	146.7	6820

are various transitional regimes. The correct form of Equation 6 is controversial. It is rigorously valid only when the gap between inner and outer cylinders is small, that is  $(r_2 - r_1) \leq (r_2 + r_1)/2$  [14, 15]. Failure in meeting this condition has led to different forms of Equation 6 cited in the literature.

Matic, Lovrecek and Skanski [15] pointed out that when the restriction imposed by the small gap is not observed, the turbulent flux character vanishes at a certain distance of the outer wall. They suggest that in this case, Prandtl thickness layer should substitute the outer cylinder radius. Accordingly, Taylor number should be calculated by the expression:

$$Ta^* = Re(\delta_{Pr}/r_1) \quad (7)$$

Using the proposed criterion, the flow is turbulent when  $Ta^* > 400$ .

In this work,  $r_1 = 1.35$  cm and  $r_2 = 5.05$  cm so that  $(r_2 - r_1)/(r_2 + r_1) \approx 0.58$ . Table 2 presents the values of the dimensionless groups and other quantities for characterization of the flow regime present in the experiments reported here. In this Table  $\delta_N$  and  $Sc$  (1690) was calculated for the HCl/Fe<sup>3+</sup> medium, considered as typical.  $\delta_N$  was calculated according to Eisenberg and others [1] and  $\delta_{Pr}$  and  $Re$  according to Matic and others [15]:

$$\delta_N = 1/(0.082 U^{0.732} d^{-0.3} \nu^{-0.344} D^{0.356}) \quad (8)$$

$$Re = Ud/\nu \quad (9)$$

$$\delta_{Pr} = \delta_N Sc^{1/3} \quad (10)$$

Inspection of Table 2 reveals that based on either criterion ( $Ta^*$  or  $Ta$ ) it can be said that the RCE operates in the turbulent flow regime in all experiments described in this paper.

### 3.5. Effect of the developed roughness on the surface of the RCE

The effect of surface roughness on mass transport in a RCE was investigated by several authors and two

approaches were considered: (a) Electrodes machined to a definite degree and pattern of roughness [9, 10, 16, 17] and (b) Naturally developed roughness by means of metal deposition [3, 4]. In these experiments, an enhancement in mass transport caused by increase in turbulence near the electrode surface has been demonstrated.

According to Kapesser and others [9] and Makrides and Hackerman [10] the effect of surface roughness would be an increase in mass transport and should appear in equation of RCE as an increased  $x$ . The surface protuberances with dimensions comparable to the laminar sublayer could lead to an increase in turbulence and, consequently, in  $x$  values.

The experiments related in this work were conducted using different surface roughness. The limiting current density measurements for  $\text{Fe}^{3+}$  reduction was done on a smooth surface (sanded with 600 grit sandpaper) and on a rough one (precorroded). It was assumed in this case that during each run the surface did not change. In experiments involving copper reduction and weight loss measurements, the electrode was smooth at the start and became rough towards the end of the experiment.

The surface roughness was measured in two electrode surface conditions, 600 grit sanded (0.25–0.42  $\mu\text{m}$ ) and precorroded (0.40–0.91  $\mu\text{m}$ ). According to Table 2 these values account for less than 1% of the boundary layer thickness. If these values are taken as representative, it can be concluded that the developed roughness was small and did not influence the mass transport. Then the RCE can be considered as a smooth one working in the turbulent flow regime.

#### 4. Conclusion

A rotating cylinder electrode was constructed and hydrodynamically characterized in turbulent flow using

four different electrochemical systems. The empirical relationship between rotation rate and mass transport was

$$I_L = 0.082 n F C A d^{-0.3} v^{-0.344} D^{0.644} U^{0.732}$$

within a 95% confidence level. It was verified that a moderate increase in surface roughness did not influence the mass transport process and thus the relation is valid in studies of technological importance such as corrosion and electrodeposition.

#### References

1. M. Eisenberg, C.W. Tobias and C.R. Wilke, *J. Electrochem. Soc.* **106** (1954) 306.
2. J. Pang and I.M. Ritchie, *Electrochim. Acta* **26** (1981) 1345.
3. D.R. Gabe and F.C. Walsh, *J. Appl. Electrochem.* **14** (1984) 555.
4. D.R. Gabe and F.C. Walsh, *J. Appl. Electrochem.* **14** (1984) 565.
5. D.C. Silverman and M.E. Zerr, *Corrosion* **42** (1986) 633.
6. F.P. Ijsseling, L.P.H.J. Drolenga and B.H. Kolster, *Br. Corros. J.* **17** (1982) 162.
7. R.A. Holser, G. Prentice, R.B. Pond Jr and R. Guanti, *Corrosion* **46** (1990) 764.
8. J.W. Burgman and P.J. Sides, *Electrochim. Acta* **34** (1989) 841.
9. R. Kapesser, I. Cornet and R. Greif, *J. Electrochem. Soc.* **118** (1971) 1955.
10. A.C. Makrides and N. Hackerman, *J. Electrochem. Soc.* **105** (1958) 1073.
11. S.L.F.A. da Costa and S.M.L. Agostinho, *J. Electroanal. Chem.* **284** (1990) 173.
12. H. Schlichting, 'Boundary Layer Theory' (McGraw-Hill, New York, 1968).
13. Y. Kawase and J.J. Ulbrecht, *Electrochim. Acta* **33** (1988) 199.
14. D.R. Gabe, *J. Appl. Electrochem.* **4** (1974) 91.
15. D.J. Matic, B. Lovrecek and D. Skanski, *J. Appl. Electrochem.* **8** (1978) 391.
16. P.A. Makanjoula and D.R. Gabe, *Surf. Technol.* **24** (1985) 29.
17. D.R. Gabe and P.A. Makanjoula, *J. Appl. Electrochem.* **17** (1987) 370.